Cell

Article

Leptin and Insulin Act on POMC Neurons to Promote the Browning of White Fat

Garron T. Dodd,[1] Stephanie Decherf,[1] Kim Loh,[1] Stephanie E. Simonds,[2] Florian Wiede,[1] Eglantine Balland,[2] Troy L. Merry,[1] Heike Münzberg,[3] Zhong-Yin Zhang,[4] Barbara B. Kahn,[5] Benjamin G. Neel,[6] Kendra K. Bence,[7] Zane B. Andrews,[2] Michael A. Cowley,[2] and Tony Tiganis[1,*]

[1]Department of Biochemistry and Molecular Biology, Monash University, Victoria 3800, Australia
[2]Department of Physiology, Monash University, Victoria 3800, Australia
[3]Pennington Biomedical Research Center, LSU Systems, Baton Rouge, LA 70808, USA
[4]Department of Biochemistry and Molecular Biology, Indiana University School of Medicine, Indianapolis, IN 46202, USA
[5]Division of Endocrinology, Diabetes and Metabolism, Department of Medicine, Beth Israel Deaconess Medical Center and Harvard Medical School, Boston, MA 02215, USA
[6]Campbell Family Cancer Research Institute, Ontario Cancer Institute, Princess Margaret Hospital and Department of Medical Biophysics, University of Toronto, Toronto, ON M5G 2M9, Canada
[7]Department of Animal Biology, School of Veterinary Medicine, University of Pennsylvania, Philadelphia, PA 19104, USA
*Correspondence: tony.tiganis@monash.edu
http://dx.doi.org/10.1016/j.cell.2014.12.022

SUMMARY

The primary task of white adipose tissue (WAT) is the storage of lipids. However, "beige" adipocytes also exist in WAT. Beige adipocytes burn fat and dissipate the energy as heat, but their abundance is diminished in obesity. Stimulating beige adipocyte development, or WAT browning, increases energy expenditure and holds potential for combating metabolic disease and obesity. Here, we report that insulin and leptin act together on hypothalamic neurons to promote WAT browning and weight loss. Deletion of the phosphatases PTP1B and TCPTP enhanced insulin and leptin signaling in proopiomelanocortin neurons and prevented diet-induced obesity by increasing WAT browning and energy expenditure. The coinfusion of insulin plus leptin into the CNS or the activation of proopiomelanocortin neurons also increased WAT browning and decreased adiposity. Our findings identify a homeostatic mechanism for coordinating the status of energy stores, as relayed by insulin and leptin, with the central control of WAT browning.

INTRODUCTION

There are two types of adipose tissue in humans, white adipose tissue (WAT) and brown adipose tissue (BAT). WAT can store vast amounts of chemical energy as triglycerides (TAGs) for utilization during periods of fasting or starvation. In contrast, BAT dissipates the chemical energy stored in TAGs as heat to preserve core temperature during hypothermia and to counteract obesity (Rosen and Spiegelman, 2014). Brown adipocytes contain a high density of mitochondria with high amounts of uncoupling protein-1 (UCP-1) allowing for the uncoupling of fatty acid oxidation from ATP production to generate heat (Rosen and Spiegelman, 2014). Although BAT was initially considered to be present only in infants, it is now established that substantial depots of UCP-1 expressing brown-like fat can be detected in the supraspinal, supraclavicular, pericardial, and neck regions of adult humans (Cypess et al., 2009; van Marken Lichtenbelt et al., 2009; Virtanen et al., 2009). These brown-like fat depots can be induced in response to cold, but their abundance is diminished in older and obese subjects (Lee et al., 2014; Ouellet et al., 2011).

Brown-like fat is also found in rodents and is composed of beige adipocytes interspersed among white adipocytes (Rosen and Spiegelman, 2014). Under basal conditions, beige adipocytes express little to no UCP-1, but UCP-1 induction in response to cold promotes thermogenesis and energy expenditure (Rosen and Spiegelman, 2014). Interestingly, the interscapular BAT in human infants is similar to classical brown fat in rodents (Lidell et al., 2013), whereas the brown-like fat in adult humans has a molecular signature reminiscent of rodent beige fat (Lidell et al., 2013; Wu et al., 2012). Increasing WAT browning in rodents increases energy expenditure and suppresses diet-induced obesity and glucose intolerance (Seale et al., 2011). On the other hand, preventing WAT browning by deleting *Prdm16*, a transcriptional cofactor that increases UCP-1 expression, promotes obesity and severe insulin resistance (Cohen et al., 2014; Seale et al., 2011). Understanding the molecular processes governing WAT browning is highly significant, as this may identify novel approaches for increasing energy expenditure and combating obesity and the metabolic syndrome. Efforts to date have focused primarily on the role of factors that act directly on beige preadipocytes, such as irisin and FGF21 (Boström et al., 2012; Lee et al., 2014). However, there is mounting evidence that the central nervous system (CNS) control of WAT browning is also important (Plum et al., 2007; Ruan et al., 2014; Williams et al., 2014).

Leptin is produced by adipocytes and is critical for energy homeostasis and body weight control. Leptin receptors (LEPRs) are expressed in distinct regions of the brain, including the arcuate nucleus (ARC) of the hypothalamus (Myers et al.,

2008). The ARC contains two opposing neuronal populations: the appetite-suppressing proopiomelanocortin (POMC) and the orexigenic neuropeptide Y (NPY) and agouti-related peptide (AgRP)-neuropeptide-expressing neurons (Cowley et al., 2001; Elias et al., 1999). Leptin acts on POMC and NPY/AgRP neurons to suppress food intake and promote energy expenditure (Myers et al., 2008). One mechanism by which leptin increases energy expenditure is through the promotion of BAT thermogenesis. Leptin action in the hypothalamus increases sympathetic nerve activity (SNA) to BAT, increasing both UCP-1 expression and BAT activity (Commins et al., 2000; Morrison et al., 2014). Leptin signals via the LEPR to activate Janus-activated kinase (JAK)-2, which promotes signaling via effector cascades, including the phosphatidyinositol 3-kinase (PI3K)/AKT and signal transducer and activator of transcription (STAT)-3 pathways, to increase *Pomc* expression and inhibit *Agrp* expression (Myers et al., 2008). The principal role of the melanocortin system in body weight control is underscored by the marked obesity in humans and rodents with null mutations in the leptin, LEPR, or POMC genes (Coll et al., 2004).

Another peripheral factor affecting the melanocortin system is insulin (Varela and Horvath, 2012). Insulin is released from pancreatic β cells following a rise in blood glucose and acts via the insulin receptor (IR) tyrosine kinase and the PI3K/AKT pathway in liver, muscle, and fat to lower blood glucose levels (Saltiel and Kahn, 2001). Insulin also acts in the ARC on POMC and AgRP/NPY neurons to regulate whole-body glucose metabolism and elicit anorectic responses (Benoit et al., 2002; Brüning et al., 2000; Könner et al., 2007). One prevailing view is that different POMC neurons exist and that leptin and insulin may act on distinct POMC neuronal subsets (Hill et al., 2010; Sohn et al., 2011; Williams et al., 2010).

The protein tyrosine phosphatases PTP1B (*PTPN1*) and TCPTP (*PTPN2*) regulate body weight and glucose homeostasis (Tiganis, 2013). PTP1B dephosphorylates JAK2 to suppress leptin signaling in hypothalamic neurons, including POMC neurons (Banno et al., 2010; Bence et al., 2006; Tiganis, 2013), whereas TCPTP dephosphorylates STAT3 in the hypothalamus (Loh et al., 2011). We have taken advantage of mice lacking PTP1B, TCPTP, or both phosphatases in POMC neurons to demonstrate that PTP1B and TCPTP selectively regulate leptin and insulin signaling to affect body weight, energy expenditure, and peripheral glucose homeostasis. We report that the combined inactivation of PTP1B and TCPTP and the promotion of leptin and insulin signaling in POMC neurons increases WAT browning and energy expenditure and prevents the development of diet-induced obesity. Our findings identify a mechanism in which POMC neurons integrate insulin and leptin feedback to drive WAT browning and maintain energy homeostasis.

RESULTS

Decreased Adiposity in POMC-TC Mice

Previous studies have established that PTP1B regulates leptin signaling in POMC neurons (Banno et al., 2010), but the precise neuronal populations in which TCPTP exerts its effects remain unknown. Thus, we assessed TCPTP versus GFP expression in the hypothalami of *Pomc*-GFP transgenic mice (Figures 1A and S1A available online). TCPTP protein was detected in 28.3% ± 5.9% of all GFP-positive POMC neurons in the ARC with colocalization predominating in the central-caudal ARC (Figure 1B), where both LEPR- and IR-responsive POMC neurons have been detected (Williams et al., 2010). No TCPTP staining was detected in the rostral ARC (Figures 1B and S1B). TCPTP colocalization with GFP-expressing POMC neurons was confirmed by flow cytometry in papain-digested hypothalami (Figure 1C). LEPR-responsive POMC neurons are also found in the nucleus of the solitary tract (NTS) in the hindbrain. Although TCPTP expression was evident in the NTS, the majority of TCPTP staining did not colocalize with GFP-expressing POMC neurons (Figure S1C).

Next, we examined the localization of PTP1B in POMC neurons in the ARC and its coincidence with TCPTP (Figures 1D–1F and S1A). PTP1B was detected in 74.8% ± 11.2% of all GFP-positive POMC neurons in the ARC, with PTP1B/GFP colocalization predominating in the central-caudal ARC (Figure 1E). In contrast to TCPTP, PTP1B was also expressed in the rostral ARC (Figure S1B). Moreover, PTP1B expression in the central-caudal ARC was not restricted to medial POMC neurons, where it largely coincided with TCPTP (Figure 1F) but was also found in lateral POMC neurons, where TCPTP expression was not evident (Figures 1B, 1E, and 1F). Also, TCPTP, but not PTP1B, was expressed in a subset of medial-caudal POMC neurons (Figure 1F). Thus, TCPTP and PTP1B are found in both overlapping and distinct POMC neuronal subsets in the ARC.

To determine whether TCPTP might function in the melanocortin pathway, we crossed *Ptpn2*$^{fl/fl}$ mice (Loh et al., 2011) with *Pomc*-Cre transgenic mice to excise *Ptpn2* (*Pomc*-Cre;*Ptpn2*$^{fl/fl}$: POMC-TC) in POMC-expressing neurons (Figures S1D and S1E). We compared these mice to PTP1B POMC neuronal cell-specific knockout mice (*Pomc*-Cre;*Ptpn1*$^{fl/fl}$: POMC-1B), generated as described previously (Banno et al., 2010). To visualize POMC cell-specific Cre-mediated recombination, we crossed POMC-TC mice to *Z/EG* reporter mice that express GFP after Cre-mediated recombination (Figure 1G). *Z/EG*;POMC-TC mice expressed GFP in the ARC and this overlapped with 92% of POMC-expressing cells (Figures 1G and 1H); no GFP staining was evident in non-POMC cells. As reported for POMC-1B mice (Banno et al., 2010), no differences were evident in the number of hypothalamic POMC neurons in POMC-TC mice (Figure 1I). POMC is expressed in the ARC, as well as the pituitary and the NTS in the hindbrain. In addition, ARC POMC neurons project to the lateral reticular nucleus in the brainstem. Consistent with this, the recombined *Ptpn2* allele (Δ*Ptpn2*) in POMC-TC mice was evident in whole-brain, hypothalamic, pituitary, and hindbrain DNA extracts, but not in liver extracts (Figure S1D). As expected, differences in TCPTP protein were not observed in the hypothalamic extracts of POMC-TC versus control mice (Figure S1E) because POMC neurons constitute only a small proportion of the total hypothalamic cell population (Cowley et al., 2001).

Body weights were not altered in POMC-TC or POMC-1B versus floxed controls (Figures 2A, 2B, and S2A). Nevertheless,

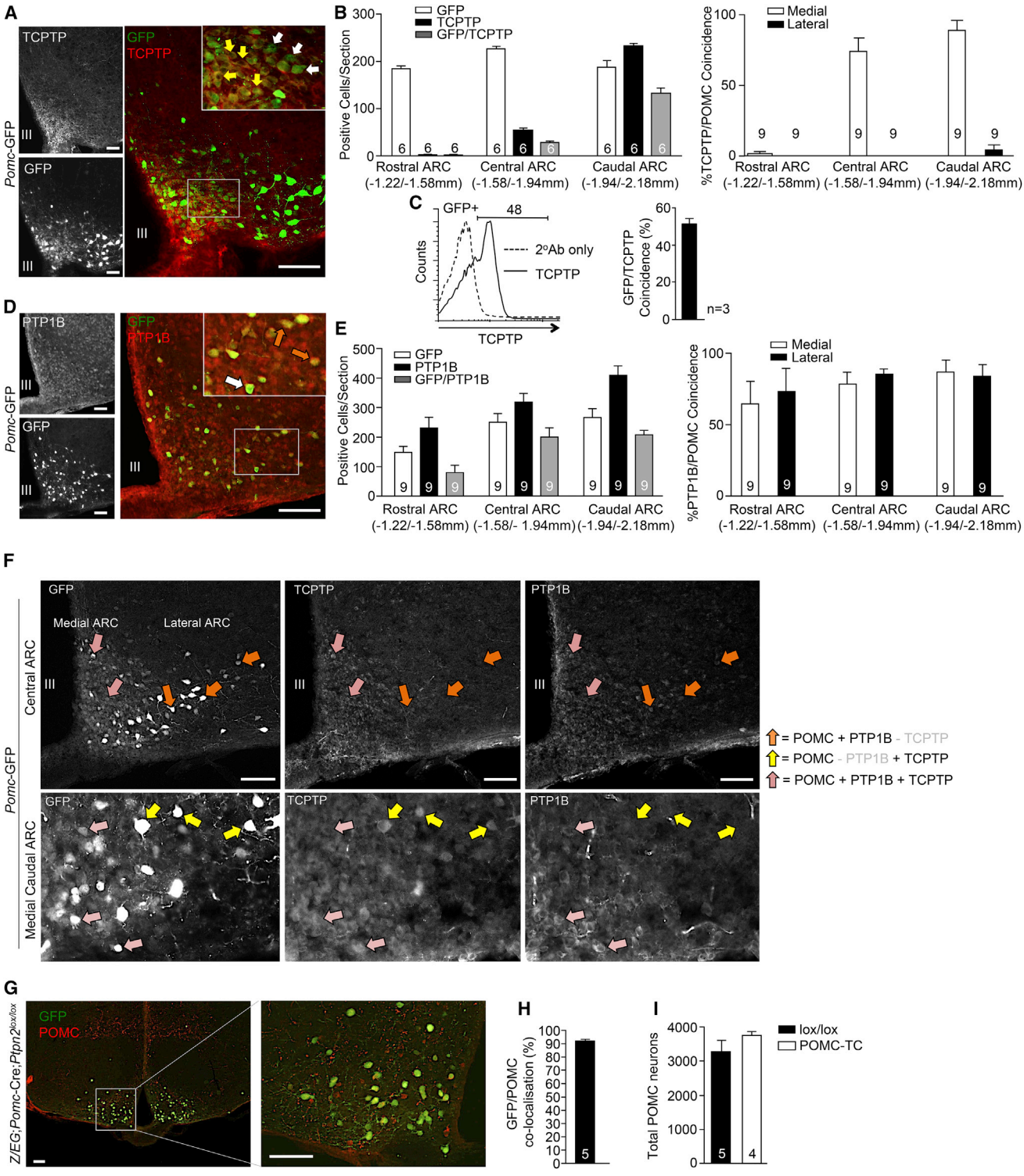

Figure 1. TCPTP and PTP1B in POMC Neurons

(A) Immunostaining for TCPTP in GFP-positive ARC POMC neurons.

(B) Rostral-caudal immunostaining quantification of GFP- and TCPTP-expressing ARC cells.

(C) Papain-digested hypothalami of *Pomc*-GFP mice were analyzed by flow cytometry for GFP and TCPTP.

(D) Immunostaining for PTP1B in GFP-positive ARC POMC neurons.

(legend continued on next page)

epididymal and subcutaneous fat pad weights were decreased in POMC-TC mice and variably decreased in POMC-1B mice; only epididymal fat was significantly decreased in POMC-1B mice (Figures 2A and 2B). Dual-energy X-ray absorptiometry (DEXA) revealed that whole-body adiposity was significantly decreased in POMC-TC mice, but not in POMC-1B mice (Figures 2A and 2B). Neither bone mineral densities nor lean masses were altered (Figures 2A and 2B), and body lengths and liver weights were similar in both groups (Figures S2B and S2C). Previous studies have established that PTP1B deletion in the pituitary (*Cga*-Cre;*Ptpn1*$^{lox/lox}$) does not impact on body weight (Banno et al., 2010). Similarly, we found that TCPTP deletion in the pituitary (*Cga*-Cre;*Ptpn2*$^{lox/lox}$) did not result in overt differences in body weight or adiposity (Figures S2D–S2H). The differences in adiposity in POMC-TC and POMC-1B mice could not be ascribed to alterations in food intake, energy expenditure, or activity, and there were no differences in fuel utilization (assessed by respiratory exchange ratio, RER) in either group (Figures S2I and S2J). These findings are consistent with previous studies reporting that LEPR or IR deficiencies in POMC neurons do not alter food intake or RER (Balthasar et al., 2004; Berglund et al., 2012; Hill et al., 2010; Könner et al., 2007).

PTP1B, but Not TCPTP, Regulates Leptin Sensitivity

The deletion of TCPTP or PTP1B in neural and glial cells by Cre-LoxP recombination using the *Nes*-Cre transgene enhances leptin sensitivity and protects mice from diet-induced obesity (DIO) (Loh et al., 2011). Accordingly, we assessed whether the decreased adiposity in chow-fed POMC-TC and POMC-1B mice might be ascribed to enhanced leptin sensitivity. POMC-TC, POMC-1B, or floxed control mice were administered leptin intraperitoneally (IP) for 3 days, and body weights and overnight food intake were recorded. Surprisingly, deletion of TCPTP in POMC neurons did not alter the leptin-mediated attenuation of food intake or decrease in body weight (Figures 2C and S2K), despite the fact that 86.5% ± 6.5% of LEPR-positive ARC POMC neurons express TCPTP (Figure S1E). In addition, plasma leptin levels (Figure 2D), leptin-induced STAT3 Y705 phosphorylation (p-STAT-3; Figures S2L and S2M), and leptin-induced hypothalamic *Pomc* expression (Figure 2G) were not altered by TCPTP deficiency, which is consistent with unaltered leptin sensitivity. As reported previously (Banno et al., 2010), PTP1B deficiency enhanced the leptin-mediated repression of body weight (Figure 2E) without overt changes in food intake (Figure S2K), reduced fed plasma leptin levels (Figure 2F), and significantly increased leptin-induced hypothalamic p-STAT-3 and *Pomc* expression (Figures 2G, S2N, and S2O); as expected, there were no differences in *Agrp* and *Npy* expression (Figure S2P). Thus, the reduced adiposity in POMC-TC mice is independent of changes in leptin sensitivity.

TCPTP, but Not PTP1B, Regulates Insulin Signaling

PTP1B and TCPTP dephosphorylate the IR and attenuate insulin signaling in the periphery (Tiganis, 2013). As the CNS effects of leptin and insulin overlap, and hypothalamic IR activation alters peripheral lipid and glucose metabolism (Marino et al., 2011; Plum et al., 2006), we monitored the effects of TCPTP versus PTP1B deficiency on hypothalamic insulin signaling. First, we determined whether PTP1B versus TCPTP deficiency in POMC neurons enhanced insulin-induced PI3K/AKT signaling in the ARC by monitoring AKT Ser-473 phosphorylation (p-AKT) by immunohistochemistry. TCPTP, but not PTP1B, deficiency enhanced p-AKT staining in the ARC in response to insulin (Figures 2H–2J). In keeping with the selective effects on p-AKT signaling, insulin-induced hypothalamic *Pomc* expression was significantly enhanced in POMC-TC, but not in POMC-1B mice (Figure 2K). To independently assess TCPTP's capacity to regulate insulin signaling in POMC neurons, we also took advantage of a highly specific TCPTP inhibitor, compound 8 (Zhang et al., 2009). This inhibitor is highly selective for TCPTP over PTP1B and intracerebroventricular (ICV) compound 8 administration enhances leptin signaling and sensitivity in wild-type mice, but not neuronal cell-specific TCPTP knockout mice (Loh et al., 2011). Compound 8 or aCSF (artificial cerebrospinal fluid) vehicle control were administered ICV into fasted C57BL/6 mice that were subsequently injected with insulin and hypothalami extracted for analysis by real-time PCR. Administration of compound 8 increased insulin-induced *Pomc* expression by ~2.5-fold (Figure 2L). Taken together, these results demonstrate that TCPTP attenuates insulin signaling in POMC neurons.

Decreased Adiposity and Increased Energy Expenditure in DKO Mice

Our results indicate that PTP1B and TCPTP differentially contribute to leptin and insulin signaling in POMC neurons. Hence, we generated POMC-TC and POMC-1B double-knockout (DKO) mice to examine whether the combined increase in IR and LEPR signaling in POMC neurons affects body weight and glucose metabolism. DKO mice had a modest reduction in body weight at 10 weeks of age, but body length, liver weight, lean mass, and bone density were unaltered (Figures 3A–3C). Differences in body weight could be explained by reduced whole-body adiposity (Figures 3B and 3C). The reduction in body weight and adiposity in DKO mice was accompanied by increased dark-phase energy expenditure without significant changes in ambulatory activity or RER or changes in food intake or feeding efficiency (Figure 3D). Furthermore, leptin sensitivity, as assessed by the effects of leptin on body weight (Figure 3E) or inferred by the reduced fed plasma leptin levels, was improved in DKO mice (Figure 3F). This was accompanied by increased leptin-induced hypothalamic *Pomc* expression in DKO mice (Figure 3G). Finally, insulin-induced

(E) Rostral-caudal immunostaining quantification of GFP- and PTP1B-expressing ARC cells.
(F) Immunostaining for PTP1B and TCPTP in GFP-positive POMC neurons in the ARC.
(G–I) (G) Immunostaining and (H and I) quantification of ARC GFP and POMC colocalization and the total number of ARC POMC neurons in *Z/EG*;POMC-TC mice. Representative images of three or more experiments are shown. Data are means ± SEM for the indicated number of mice (30 sections/mouse) or (C) experimental repeats.

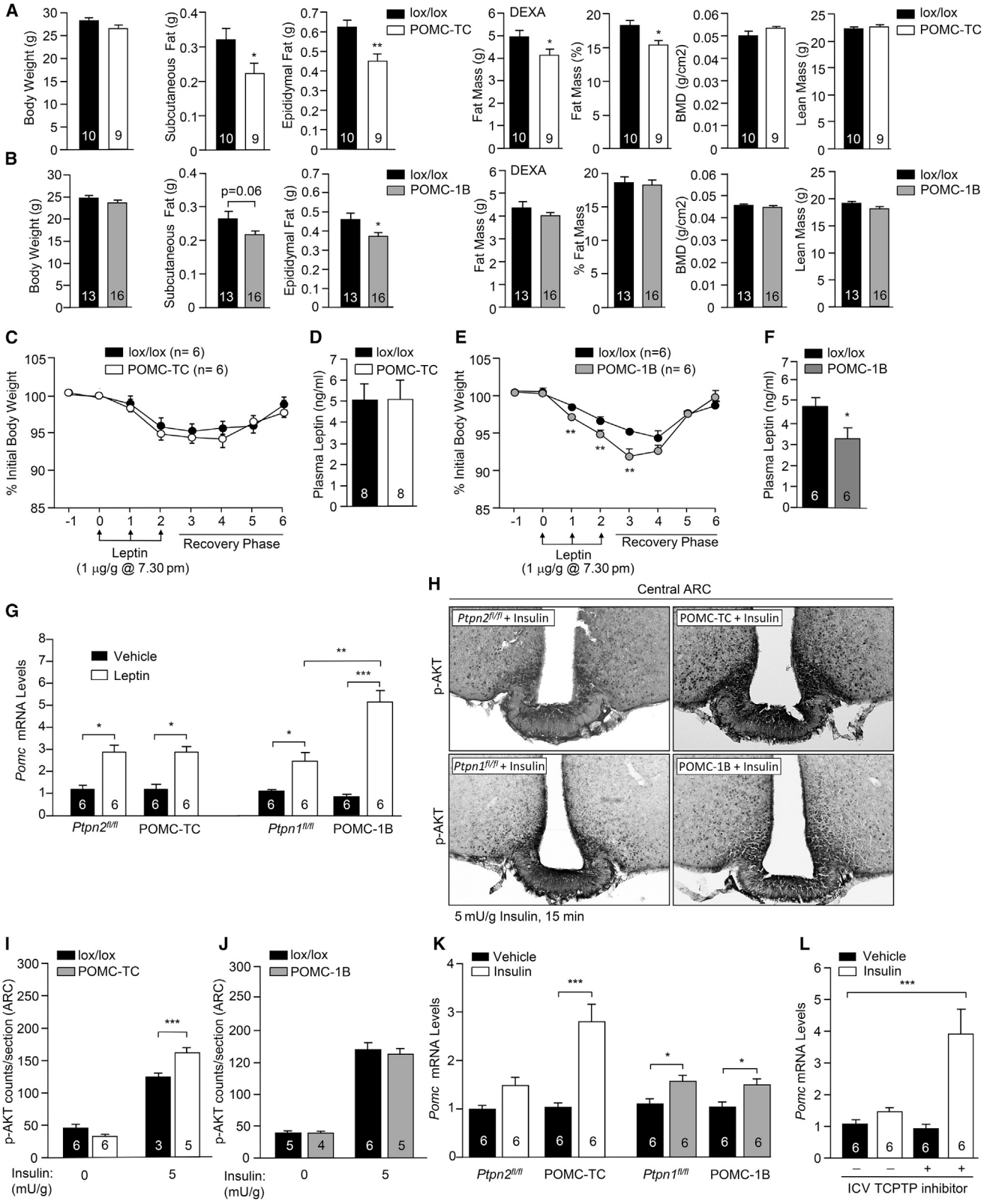

(legend on next page)

hypothalamic *Pomc* expression was also increased in DKO mice (Figure 3H). These results are consistent with combined deficiencies in PTP1B and TCPTP promoting both central leptin and insulin signaling in POMC neurons to attenuate body weight/adiposity.

Increased BAT Thermogenesis and WAT Browning in DKO Mice

As the decreased adiposity and increased energy expenditure in chow-fed DKO mice could not be accounted for by changes in food intake or ambulatory activity, we examined whether DKO mice had elevated BAT thermogenesis and/or WAT browning. Although interscapular BAT mass was not altered (Figure S3A), *Ucp-1* gene expression was increased by more than 3-fold in DKO mice, which is consistent with increased BAT activity (Figure 4A); BAT *Ucp-1* expression was not altered in POMC-TC or POMC-1B mice (Figure 4A). Indeed, BAT thermogenesis, as assessed with sensors implanted below interscapular BAT, was increased during the light phase (when mice are less active) in DKO mice, but not in POMC-TC or in POMC-1B mice (Figure 4B). On the other hand, core temperature was not different from controls (Figure S3B), which is consistent with normal whole-body thermoregulation.

To determine whether WAT browning was also elevated in DKO mice, we measured *Ucp-1* gene expression in epididymal, inguinal, mesenteric, and infrarenal fat (Figure 4A). We found that *Ucp-1* expression was increased by 15- to 20-fold, specifically in inguinal WAT in DKO mice; inguinal *Ucp-1* expression was not altered in POMC-TC or POMC-1B mice (Figure 4A). Elevated *Ucp-1* mRNA in the inguinal fat of DKO mice was accompanied by increases in UCP-1 protein (Figures 4C and 4D). Inguinal fat in DKO mice had a distinct histological (hematoxylin and eosin [H&E] staining) morphology (Figure 4E), characterized by the presence of small adipocyte clusters with a multilocular lipid droplet morphology, a characteristic of brown fat (Rosen and Spiegelman, 2014). WAT browning in DKO mice also was accompanied by increased expression of *Prdm16* and *Cidea* (Figure 4F), which are found in brown and beige adipocytes, and *Tmem26* and *Cd137* (Figure 4F), which are specific to beige adipocytes (Wu et al., 2012). Previous studies have shown that cold-induced WAT browning is associated by increased angiogenesis (Xue et al., 2009). We found that angiogenesis, assessed with the angiogenesis marker CD34, was significantly elevated in inguinal WAT in DKO mice (Figures S3C and S3D). Together, these results demonstrate that the combined deletion of PTP1B and TCPTP in POMC neurons drives BAT thermogenesis and WAT browning.

SNA-Dependent WAT Browning Decreases Adiposity

To determine whether the increased WAT browning in DKO mice might be associated with SNA resulting from the combined deletion of PTP1B and TCPTP in POMC neurons, we assessed tyrosine hydroxylase (TH) expression in the inguinal fat of chow-fed DKO versus control mice. TH is the rate-limiting enzyme in catecholamine synthesis and is a marker of sympathetic innervation and was elevated in the inguinal fat of DKO mice (Figures S3E and S3F). Next, to determine whether the increased SNA was responsible for the WAT browning, we asked whether sympathetic denervation might attenuate WAT browning in DKO mice. To this end, we injected the neurotoxin 6-hydroxydopamine (6-OHDA) unilaterally into the inguinal fat area of 10 week-old DKO mice and monitored for changes in browning 2 weeks later. Unilateral sympathetic denervation dramatically reduced TH staining and attenuated WAT browning when compared with the contralateral fat pad, as assessed by gross morphology, the expression of browning genes (*Ucp-1*, *Prdm16*, *Cidea*) and histology/UCP-1 immunohistochemistry (Figures 5A–5C) without affecting BAT *Ucp-1* expression (Figure 5D). Indeed, sympathetic denervation reverted the increased inguinal WAT *Ucp-1* levels in DKO mice to levels comparable to floxed control mice (Figure 5E). These results indicate that WAT browning in DKO mice is dependent on SNA, rather than changes in metabolism or circulating factors associated with the decreased adiposity.

Next, we sought to determine the extent to which the increased SNA to inguinal fat and consequent browning may contribute to the increased energy expenditure and decreased adiposity in DKO mice. We first asked whether WAT browning and/or BAT activity might precede the decreased body weight/adiposity evident in DKO mice. Increased WAT browning was evident as early as 4 weeks of age, prior to any differences in body weight or adiposity (Figures 4C, 4E, 4F, and 4H). Moreover, the increased WAT browning in 4-week-old mice preceded changes in BAT activity, as assessed by the expression of *Ucp-1* (Figure 4G). To directly test that WAT browning decreased adiposity in DKO mice, we bilaterally denervated the inguinal fat pads of chow-fed DKO mice using 6-OHDA and measured the effect on adiposity and browning after 5 weeks. Strikingly, sympathetic denervation in DKO mice (assessed by TH staining; Figure S3G) resulted in increased weight gain and adiposity (Figures 5F, 5G, and S4A). Importantly, the increased adiposity in denervated DKO mice was accompanied by decreased WAT browning and a reduction in energy expenditure (Figures 5H and 5I), without alterations in RER or ambulatory activity (Figure S4B). Moreover, the increased weight gain occurred despite BAT

Figure 2. TCPTP and PTP1B Regulate Insulin and Leptin Signaling

(A and B) Body and WAT weights and body composition in 10-week-old POMC-TC, POMC-1B, and lox/lox mice.

(C and E) POMC-TC, POMC-1B, and lox/lox mice were administered leptin, and body weights were monitored.

(D and F) Fed plasma leptin levels in 8-week-old mice.

(G) Hypothalamic *Pomc* gene expression in mice injected IP saline or leptin (1 μg/g, 2 hr).

(H–J) p-AKT immunostaining in mice injected IP saline or insulin (5 mU/g, 15 min).

(K) Hypothalamic *Pomc* gene expression in mice injected IP saline or insulin (0.85 mU/g, 2 hr).

(L) Hypothalamic *Pomc* gene expression in C57BL/6 mice administered saline or insulin (0.85 mU/g, IP, 2 hr), followed by aCSF or TCPTP inhibitor (1.5 μl 0.2 nmol compound 8, ICV). Results are means ± SEM and are representative of three independent experiments; significance was determined using (C, E, G–L) two-way ANOVA.

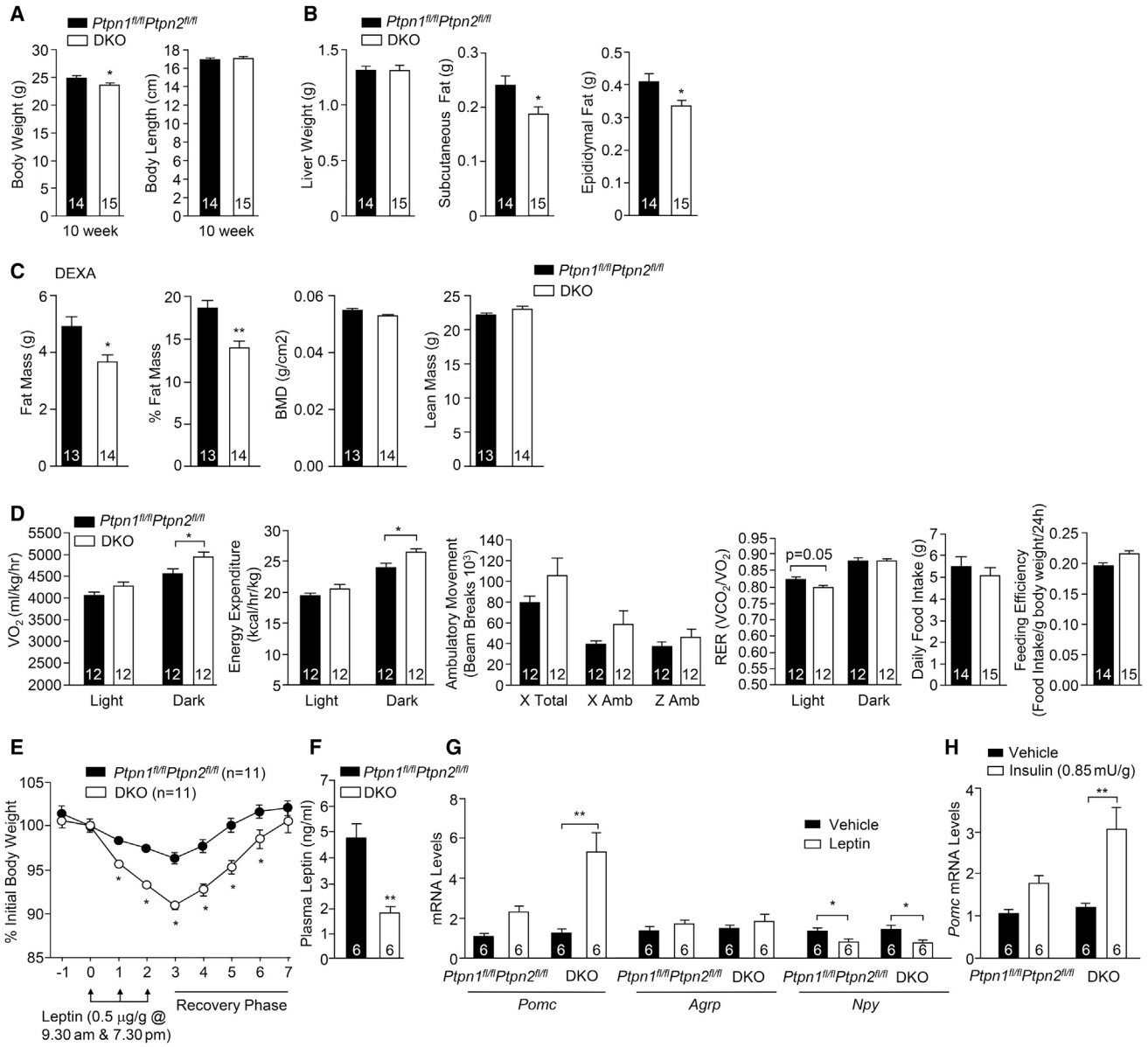

Figure 3. Decreased Adiposity and Increased Energy Expenditure in DKO Mice

(A–D) (A) Body weight and body length; (B) tissue weights; (C) body composition; and (D) oxygen consumption, energy expenditure, ambulatory activity, RER, daily food intake, and feeding efficiency in 8- to 10-week-old DKO and *Ptpn1*$^{fl/fl}$*Ptpn2*$^{fl/fl}$ mice.

(E) Mice were administered leptin and body weights recorded.

(F) Fed plasma leptin levels in 8-week-old mice.

(G and H) Hypothalamic gene expression in fasted mice injected with IP saline, (G) leptin (1 μg/g), or (H) insulin. Results are means ± SEM and are representative of at least two independent experiments; significance was determined (D, E, G, and H) using two-way ANOVA.

activity remaining elevated in DKO mice (Figure 5H). Taken together, these results causally link the increased energy expenditure and decreased adiposity in DKO mice to the elevated WAT browning.

DKO Mice Are Resistant to DIO

To assess the impact of combined PTP1B and TCPTP deficiencies in POMC neurons and increased WAT browning on DIO, we administered a high-fat diet to POMC-TC, POMC-1B, or DKO mice for 12 weeks and monitored the effects on body weight and glucose metabolism (Figures 6, S5, S6, and S7). DKO mice exhibited a significant reduction in weight gain and a marked reduction in adiposity (Figures 6A–6C and S7A). By contrast, no differences were observed in body weight, adiposity, or energy expenditure in POMC-1B or POMC-TC mice (Figures S5A–S5D and S6A–S6D). The decreased weight

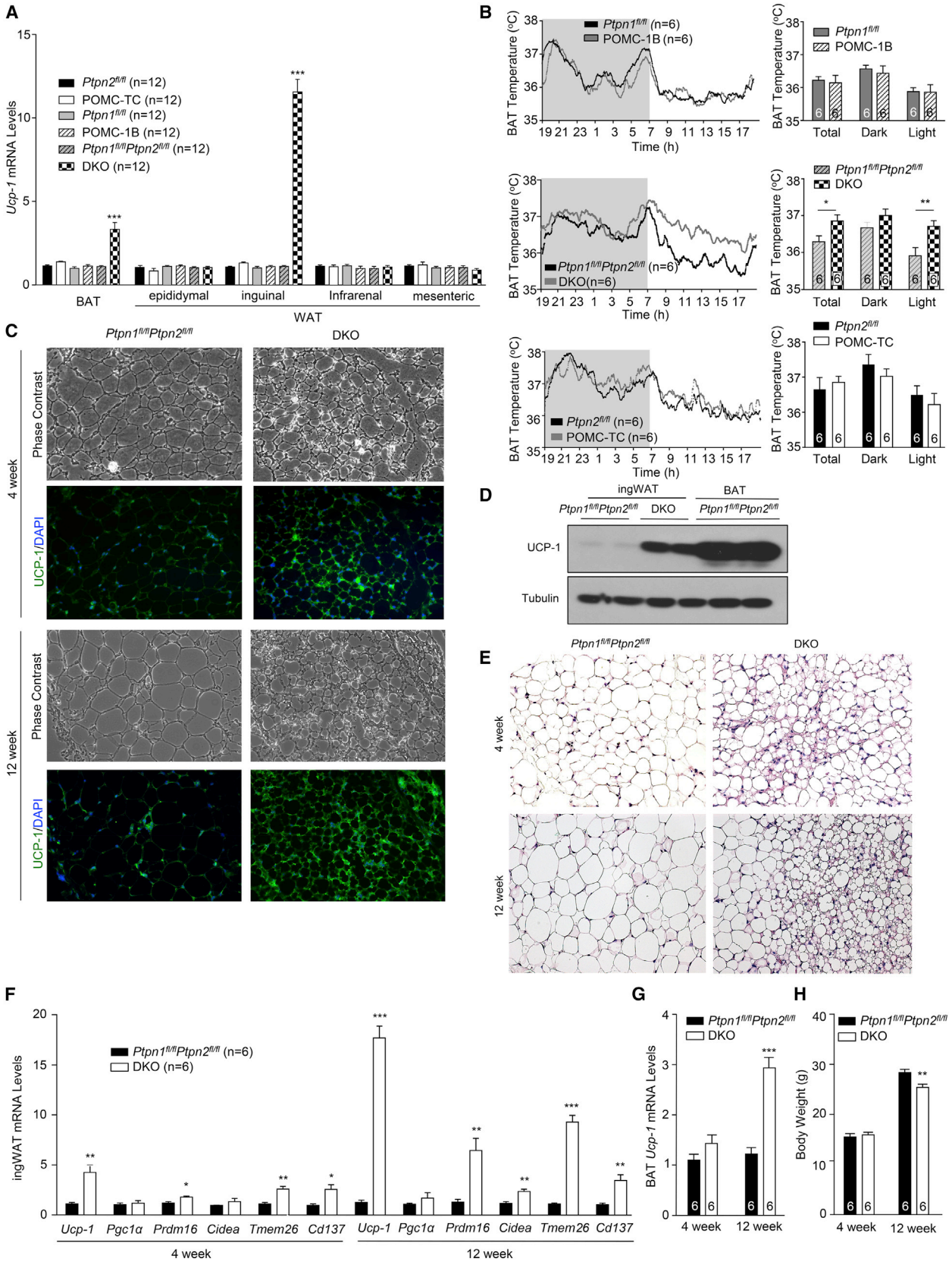

(legend on next page)

gain in DKO mice was not associated with any difference in body length, lean mass, or bone density (Figures 6C and 6D), but liver weights were significantly reduced and accompanied by a marked reduction in steatosis (Figure 6E). The decreased adiposity in high-fat-fed (HFF) DKO mice was accompanied by unaltered food intake, but feeding efficiency was increased (Figure 6F), which is consistent with improved energy utilization. Moreover, HFF DKO mice exhibited increased oxygen consumption and energy expenditure, increased ambulatory activity, and increased dark-phase RER (Figure 6F). In keeping with the resistance to DIO, DKO mice had significantly greater leptin sensitivity (Figure 6G). Moreover, DKO mice exhibited a significant reduction in fasted blood glucose levels and a trend for reduced fasted insulin levels and had improved insulin and glucose tolerances (Figures 6H–6J, S7B, and S7C), consistent with overall improved glucose homeostasis. By contrast, HFF POMC-TC and POMC-1B single-mutant mice did not exhibit any differences in glucose homeostasis and leptin sensitivity (Figures S5E–S5I and S6E–S6I). These results demonstrate that the combined deletion of PTP1B and TCPTP in POMC neurons prevents the development of DIO and the associated insulin resistance, glucose intolerance, and hepatosteatosis.

The decreased adiposity in HFF DKO mice was accompanied by elevated BAT *Ucp-1* expression and increased inguinal WAT browning (Figures 6K–6M). To determine the extent to which the increased WAT browning in DKO mice prevented DIO, we bilaterally denervated (6-OHDA) the inguinal fat of DKO mice that had been HFF for 3 weeks and measured effects on adiposity, energy expenditure, and glucose homeostasis after a further 5 weeks of high-fat feeding (Figures 6N, 6O, and S7D–S7J). Bilaterally denervating inguinal fat in HFF DKO mice increased weight gain and adiposity (Figures 6N, S7D, and S7E). The increased weight gain was associated with decreased energy expenditure and RER but no alterations in ambulatory activity or food intake (Figures 6O and S7F). Moreover, the increased weight gain in the denervated HFF DKO mice was accompanied by elevated fasted blood glucose levels, glucose intolerance, insulin resistance, and hepatosteatosis (Figures S7G–S7J). These results demonstrate that the resistance to DIO in HFF DKO mice can be attributed at least in part to increased WAT browning.

Insulin and Leptin Promote WAT Browning in DKO Mice

Our studies indicate that mice lacking PTP1B or TCPTP in POMC neurons exhibit enhanced leptin or insulin signaling, respectively, and that their combined deficiency increases WAT browning and energy expenditure to decrease adiposity. Although these results are consistent with enhanced insulin and leptin signaling driving WAT browning, they do not exclude the contribution of other pathways. Moreover, they do not exclude the possibility that the combined PTP1B and TCPTP deficiency may lead to synergistic effects on leptin-induced JAK2 activation and STAT-3 signaling, so that leptin signaling alone promotes WAT browning. To test this, we administered POMC-1B (leptin hypersensitive) or POMC-TC (insulin hypersensitive) mice either vehicle or leptin and assessed the effects on body weight, WAT browning, and BAT activity (Figures 7A and 7B). We reasoned that, if both leptin and insulin signaling are required in POMC neurons for WAT browning, then WAT browning would be greatest in the leptin-treated POMC-TC mice, as POMC-TC mice are insulin hypersensitive. On the other hand, if the exacerbation of leptin signaling by combined PTP1B and TCPTP deficiencies would be sufficient to drive browning, then this would be greatest in POMC-1B mice that are leptin hypersensitive. POMC-TC, POMC-1B, or floxed control mice were administered leptin on a daily basis for 6 days, and body weights, WAT browning, and BAT *Ucp-1* expression were assessed. POMC-1B mice exhibited the greatest decrease in body weight in response to leptin (Figure 7A). Consistent with the previously established potential for leptin to drive BAT thermogenesis, BAT *Ucp-1* was elevated in leptin-treated control mice (as compared to vehicle administered C57BL/6 mice), but this was not increased further by PTP1B or TCPTP deficiency (Figure 7B). Leptin administration also modestly increased inguinal WAT browning (Figure 7B). However, browning was greatest for leptin-treated POMC-TC mice (Figures 7B, 7C, S4C, and S4D). Thus, the enhanced insulin and leptin signaling in POMC neurons may underlie the WAT browning and consequently increased energy expenditure and decreased adiposity in DKO mice.

Insulin and Leptin Act on ARC Neurons to Drive WAT Browning

To directly assess the capacity of insulin and leptin to act synergistically in the CNS to control WAT browning, we subcutaneously implanted osmotic minipumps to ICV administer either vehicle, leptin, insulin, or leptin plus insulin into the lateral ventricle over 6 days and monitored body weight, energy expenditure, BAT activity, and WAT browning (Figures 7D–7G and S4E–S4H). We found that insulin infusion alone had no effect on food intake or body weight (Figures 7D and S4F). This is in keeping with previous studies demonstrating that the chronic ICV administration of insulin does not alter food intake or overall body weight (Koch et al., 2008). As expected, leptin decreased body weight and adiposity, and notably, this was exacerbated by the coinfusion of insulin (Figure 7D). Coinfusion of leptin and insulin did not further reduce food intake compared to leptin-only infusion (Figure S4F). To assess whether the synergistic effects of insulin and leptin on body weight may result from SNA-dependent WAT browning and/or BAT thermogenesis, we measured the expression of thermogenic genes in BAT and inguinal fat. We found (1) that BAT *Ucp-1* expression increased

Figure 4. Increased Browning in DKO Mice

(A) *Ucp-1* gene expression in BAT and WAT depots from 12-week-old POMC-1B, POMC-TC, DKO, and floxed control mice.

(B) Interscapular BAT temperature.

(C–E) Histology (H&E), immunoblotting and immunohistochemistry of inguinal WAT (ingWAT).

(F and G) IngWAT or BAT gene expression.

(H) Body weights in 4- and 12-week-old mice. Data are means ± SEM and are representative of three independent experiments; significance was determined using (A) one-way or (F, G, and H) two-way ANOVA.

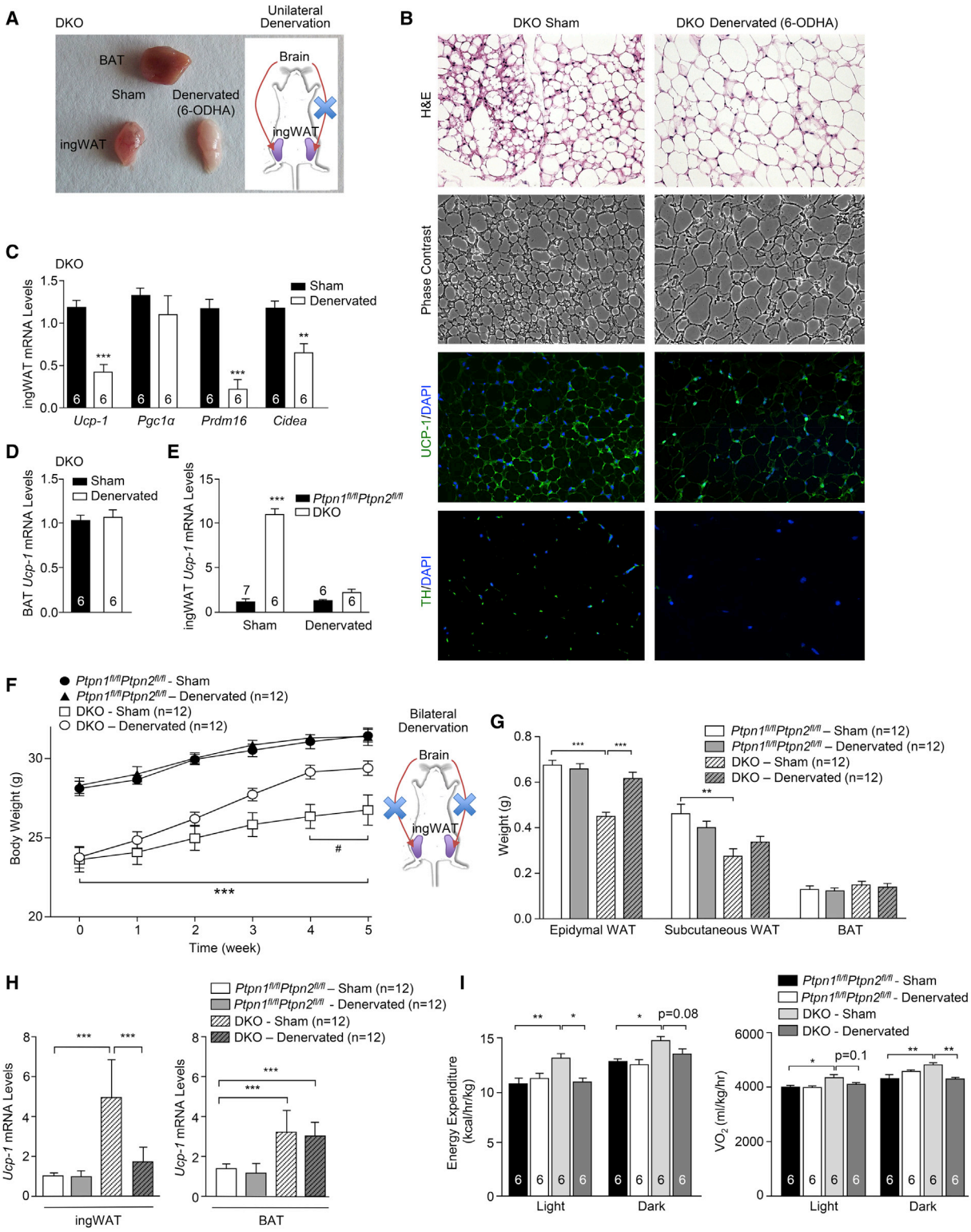

Figure 5. Denervation of DKO Inguinal WAT and Increases Body Weight

(A–D) IngWAT in 10-week-old DKO mice was unilaterally denervated (6-ODHA) and BAT and ingWAT extracted 2 weeks later for analysis. (A) Gross morphology, (B) histology/immunohistochemistry, and (C and D) gene expression; sham vehicle-administered contralateral inguinal fat pads were used as controls. (E) Contralateral sham versus denervated (6-ODHA) ingWAT from DKO versus *Ptpn1*$^{fl/fl}$*Ptpn2*$^{fl/fl}$ mice analyzed for *Ucp-1* expression.

(legend continued on next page)

similarly in response to all treatments, but not by insulin alone (Figure 7E) and (2) that leptin, but not insulin treatment alone, resulted in a modest increase in the expression of browning genes in inguinal fat (Figure 7E). In keeping with this, leptin alone modestly increased TH and UCP-1 in inguinal fat and increased whole-body energy expenditure (Figures 7F, 7G, and S4H). However, the coinfusion of leptin and insulin resulted in a marked increase in TH staining and WAT browning (Figures 7E, 7F, S4E, S4G, and S4H). Moreover, the coinfusion of leptin plus insulin resulted in a greater increase in energy expenditure than the infusion of leptin alone (Figure 7G), which is consistent with the difference in energy expenditure being attributable to increased WAT browning.

To determine the extent to which the leptin plus insulin-induced increase in energy expenditure and weight loss may be reliant on SNA-dependent WAT browning, we bilaterally denervated (6-OHDA) the inguinal fat pads of mice that were ICV infused with leptin plus insulin. We found that the increased WAT browning (*Ucp-1* expression) and energy expenditure and decreased body weight resulting from the coinfusion of leptin and insulin were significantly attenuated by the bilateral denervation of inguinal fat (Figures 7H–7J). However, the denervation did not completely prevent the increase in energy expenditure and decrease in body weight, probably because of the sustained leptin-induced activation of BAT and the suppression of food intake (Figures 7E, 7H, and 7J).

Next, we assessed whether the effects of the ICV-administered insulin and leptin on WAT browning may be mediated via neurons in the ARC. Moreover, because both insulin and leptin can signal via PI3K to depolarize and activate POMC neurons (Cowley et al., 2001; Hill et al., 2008; Qiu et al., 2010, 2014; Rahmouni et al., 2004), we determined whether the pharmacological inhibition of PI3K could suppress WAT browning. Minipumps and intra-ARC indwelling bilateral cannulas were used to infuse vehicle, leptin plus insulin or leptin, or insulin plus the PI3K inhibitor LY294002 directly into the ARC over 6 days, and effects on body weight and WAT browning were monitored (Figures 7K–7M and S4I). The infusion of leptin/insulin directly into the ARC decreased body weight and food intake and promoted WAT browning, and these effects were attenuated by LY294002 (Figures 7K–7M and S4I). Taken together, these results demonstrate that insulin and leptin act synergistically on cells in the ARC, at least in part via PI3K, to increase WAT browning and consequent energy expenditure to decrease body weight.

ARC POMC Neurons Promote WAT Browning

We next sought to understand how leptin and insulin elicit synergistic effects on ARC cells to promote WAT browning. Previous studies have provided evidence for the existence of distinct ARC POMC neurons that are differentially responsive to insulin and leptin (Hill et al., 2010; Williams et al., 2010). To determine whether insulin and leptin may promote browning by stimulating different POMC neurons, we administered mice insulin, leptin, or insulin plus leptin intraperitoneally and monitored for hypothalamic STAT3 Y705 or AKT Ser-473 phosphorylation by immunohistochemistry (Figures S4J–S4L). Leptin stimulation resulted in p-AKT and p-STAT-3 staining in both the ARC and DMH, whereas insulin increased p-AKT largely in the ARC (Figure S4J). Strikingly, insulin plus leptin stimulation resulted in p-AKT staining in ARC neurons that were devoid of p-STAT-3 (Figures S4J and S4K). At least a subset of the cells staining for p-AKT only also stained for POMC-derived α-MSH (Figure S4L). Thus, insulin and leptin can stimulate distinct neurons in the ARC. These results are consistent with the insulin plus leptin-mediated promotion of WAT browning resulting from the increased engagement of POMC neurons.

To assess whether the leptin/insulin synergy reflects the increased recruitment of POMC neurons to the melanocortin response, we sought to nonselectively activate ARC POMC neurons with the stimulatory hM3Dq DREADD (designer receptors exclusively activated by designer drugs) that is activated by clozapine-N-oxide (CNO) (Krashes et al., 2011). rAAV-hM3Dq-mCherry (capable of expressing hM3Dq-mCherry in a Cre-dependent manner) was administered into the ARC of 10-week-old *Pomc*-Cre mice that were subsequently unilaterally denervated (inguinal fat pads) with 6-OHDA. Mice were then administered vehicle or CNO to depolarize POMC neurons, and body weights and food intake were measured, and WAT browning was assessed after 14 days. CNO decreased food intake and body weight, which is consistent with POMC neuronal activation (data not shown). Postmortem analysis confirmed ARC targeting and mCherry expression in 73.1% ± 20.7% of POMC neurons (Figures S4M and S4N). CNO administration resulted in a marked increase in WAT browning in the sham-operated contralateral inquinal fat pads, but not in the 6-OHDA denervated inguinal fat pads (Figures 7N–7P). These results demonstrate that the nonselective activation of ARC POMC neurons promotes the SNA-dependent browning of inguinal WAT. This is consistent with the synergistic actions of insulin and leptin on WAT browning, reflecting the increased engagement and activation of POMC neurons.

DISCUSSION

Our studies demonstrate that leptin and insulin act synergistically on hypothalamic POMC neurons to promote WAT browning and energy expenditure to decrease adiposity. We suggest that the engagement of insulin- and leptin-responsive POMC neurons might allow for a graded melanocortin response to regulate fat stores. Leptin would elicit immediate effects on food intake, ambulatory activity, and energy expenditure by promoting BAT activity, whereas leptin and heightened postprandial insulin would act synergistically over the longer term and engage a greater proportion of POMC neurons to promote overt WAT

(F–H) 8-week-old *Ptpn1*$^{fl/fl}$*Ptpn2*$^{fl/fl}$ and DKO mice were sham operated or bilaterally denervated; (F) body weights and (G) WAT and BAT weights were assessed; and (H) ingWAT and BAT *Ucp-1* expression was measured.

(I) Energy expenditure and oxygen consumption in 24-week-old *Ptpn1*$^{fl/fl}$*Ptpn2*$^{fl/fl}$ and DKO mice 5 weeks after sham or bilateral ingWAT denervations. Data are means ± SEM and are representative of three independent experiments; significance was determined using (E and F) two-way or (G–I) one-way ANOVA. (F) * DKO v/s *Ptpn1*$^{fl/fl}$*Ptpn2*$^{fl/fl}$; # denervated DKO versus sham-operated DKO.

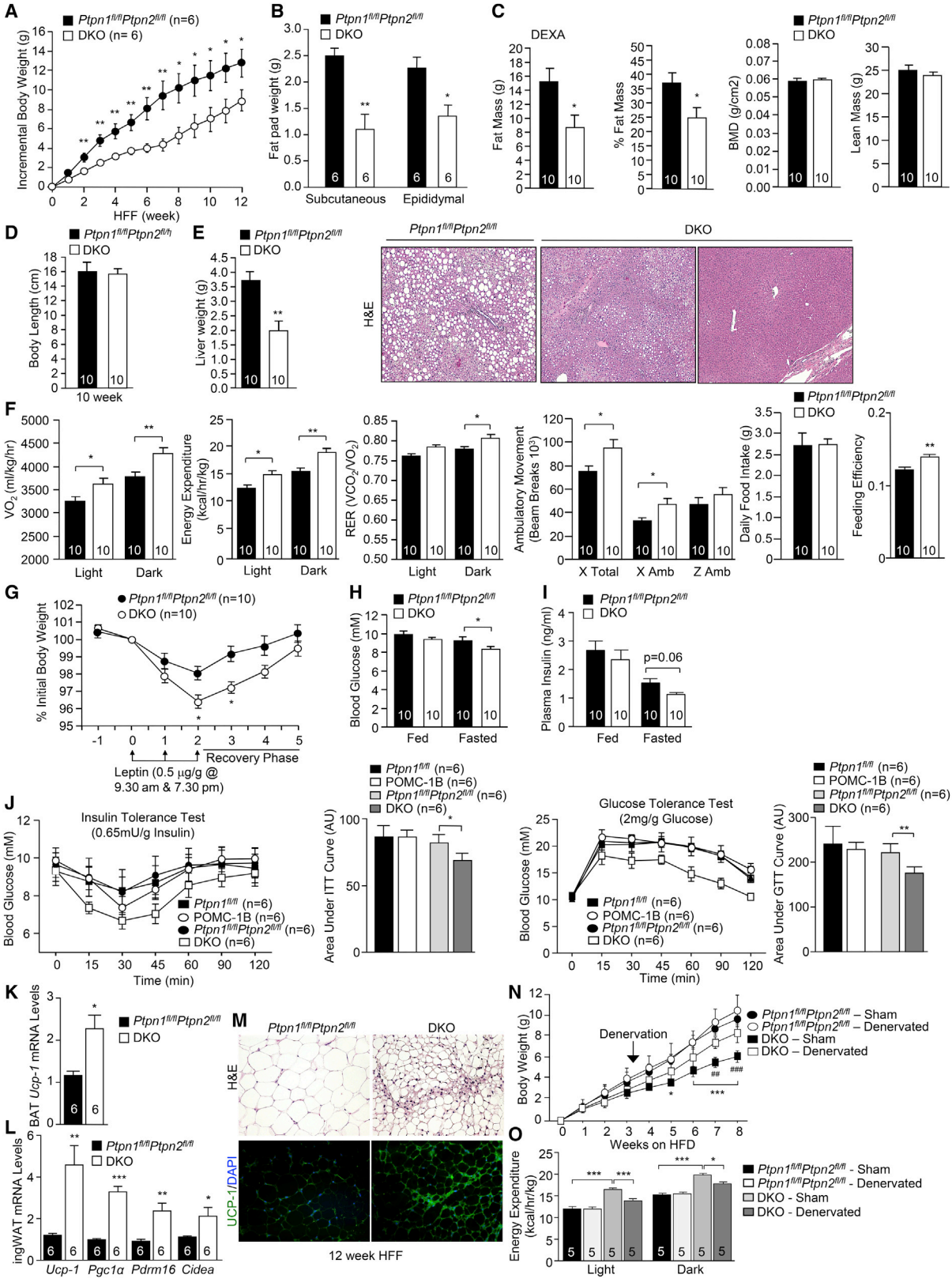

(legend on next page)

browning and increase energy expenditure to limit weight gain. This may be a major factor contributing to the ''diet-induced thermogenesis'' model of body weight control, as first described by Rothwell and Stock in 1979, whose studies involved BAT cellular expansion and differentiation in rodents eating a cafeteria diet (Rothwell and Stock, 1979).

We found that TCPTP was expressed in 30%–40% and PTP1B was expressed in 70% of ARC POMC neurons and that the two phosphatases differentially contributed to leptin and insulin signaling. Previous studies have established that both phosphatases can attenuate leptin and insulin signaling in varied cell types and tissues (Tiganis, 2013). Indeed, PTP1B attenuates insulin signaling in SF-1 neurons in the VMH (Chiappini et al., 2014), whereas neuronal TCPTP deficiency promotes hypothalamic leptin signaling in vivo (Loh et al., 2011). In this study, we found that PTP1B deficiency enhanced leptin, but not insulin signaling, and TCPTP-deficiency enhanced insulin, but not leptin signaling in POMC neurons. To some degree, the differential contributions of the phosphatases may be due to their segregation in distinct POMC neurons. Such segregation is in keeping with the existence of distinct subsets of POMC neurons in the ARC (Hill et al., 2010; Sohn et al., 2011; Williams et al., 2010). However, despite a significant degree of segregation, PTP1B and TCPTP were coexpressed in medial POMC neurons in the central-caudal ARC, and TCPTP was expressed in the majority of LEPR-expressing POMC neurons. Therefore, the impact of PTP1B versus TCPTP deficiency on leptin versus insulin signaling and that of their combined deficiencies on WAT browning and energy expenditure may also be partly ascribed to functional redundancies.

Irrespective of the roles of PTP1B and TCPTP, our findings demonstrate that both insulin and leptin are required for optimal CNS-mediated WAT browning. First, leptin administration modestly increased browning in floxed control and leptin hyperresponsive POMC-1B mice, but overt WAT browning was only evident in insulin hyperresponsive POMC-TC mice. Second, leptin or insulin ICV infusion alone had little effect on browning, whereas the coinfusion of insulin and leptin strikingly enhanced browning. By contrast, BAT activity was enhanced by 2- to 3-fold in response to leptin, but not insulin, and was not enhanced further by the coinfusion of leptin and insulin. Previous studies have implicated ARC/POMC neurons and/or leptin-induced PI3K signaling in BAT thermogenesis and WAT browning (Commins et al., 2000; Plum et al., 2007; Williams et al., 2014). However, our studies provide direct evidence for POMC neuronal activation promoting SNA-dependent WAT browning and demonstrate that insulin and leptin can act synergistically on POMC neurons to promote browning that far exceeds that achieved with leptin alone. Moreover, our studies provide evidence for the differential central control of BAT activity versus WAT browning and thus ascribe distinct physiological functions to these thermogenic tissues.

The importance of beige adipocytes to body weight control is underscored by studies overexpressing or deleting the brown adipose tissue determination factor *Prdm16* in fat (Cohen et al., 2014; Seale et al., 2011). Consistent with the importance of WAT browning for thermogenesis and energy expenditure, beige adipocytes can increase their energy uptake similar to BAT in the context of cold or β_3-adenergic stimulation (Bartelt et al., 2011). Also, the thermogenic capacity of mitochondria from the inguinal fat of cold-acclimated mice is one third of that of interscapular BAT (Shabalina et al., 2013). Our studies highlight the capacity of CNS-mediated WAT browning to regulate body weight and adiposity independently of BAT thermogenesis.

In humans, low brown and brown-like fat activity correlates with aging, obesity and diminishing metabolic health (Ouellet et al., 2011), but whether such decreases are causal or consequential and the basis for the decline remain unclear. Our results suggest that the diminishing brown-like fat may occur as a consequence of ARC cellular insulin and leptin resistance. Indeed, elevated hypothalamic PTP1B and TCPTP exacerbate cellular leptin resistance and DIO in mice (Loh et al., 2011). However, it remains to be established whether PTP1B and TCPTP are elevated in POMC neurons and whether this, along with other factors that promote cellular leptin/insulin resistance, such as SOCS3 (Mori et al., 2004), contribute to the diminished brown-like fat in obesity.

In summary, our findings define the complementary roles of TCPTP and PTP1B in central insulin and leptin signaling in POMC neurons and the synergistic central actions of insulin and leptin in the promotion of WAT browning. Our results suggest that browning may be the outcome of an integrated melanocortin response to peripheral factors that convey the status of both current (as conveyed by leptin) and anticipated energy reserves (as conveyed by increases in insulin) and highlight the potential for CNS-mediated WAT browning to regulate adiposity and combat obesity.

EXPERIMENTAL PROCEDURES

Mice

We maintained mice on a 12 hr light-dark cycle in a temperature-controlled high barrier facility with free access to food and water. Mice were fed a standard chow (4.6% fat) or a high-fat diet (23% fat; 45% of total energy

Figure 6. DKO Mice Are Resistant to DIO

(A–F) 8-week-old *Ptpn1*$^{fl/fl}$*Ptpn2*$^{fl/fl}$, and DKO mice were HFF for 12 weeks, and (A) incremental body weight, (B) fat pad weight, (C) body composition, (D) body length, (E) liver weight and histology, (F) oxygen consumption, energy expenditure, ambulatory activity, RER, food intake, and feeding efficiency were assessed.

(G–I) (G) 12 week HFF mice were administered leptin, and body weights were monitored. Fed and fasted (H) blood glucose and (I) plasma insulin levels in 12 week HFF mice.

(J) Insulin and glucose tolerance tests in 12 week HFF mice.

(K–M) (K and L) BAT or ingWAT gene expression, (M) ingWAT histology, and immunohistochemistry from 12 week HFF mice.

(N and O) *Ptpn1*$^{fl/fl}$*Ptpn2*$^{fl/fl}$ and DKO mice were HFF and either sham operated or bilaterally denervated after 3 weeks; high-fat feeding was continued for 5 weeks; and (N) incremental body weights and (O) energy expenditure were measured. Results are means ± SEM for the indicated number of mice and are representative of three independent experiments; significance was determined using (A, B, F, G, I, J, N, and O) two-way ANOVA. (N) Asterisk (*) indicates floxed v/s DKO sham operated; pound (#), DKO sham versus DKO denervated.

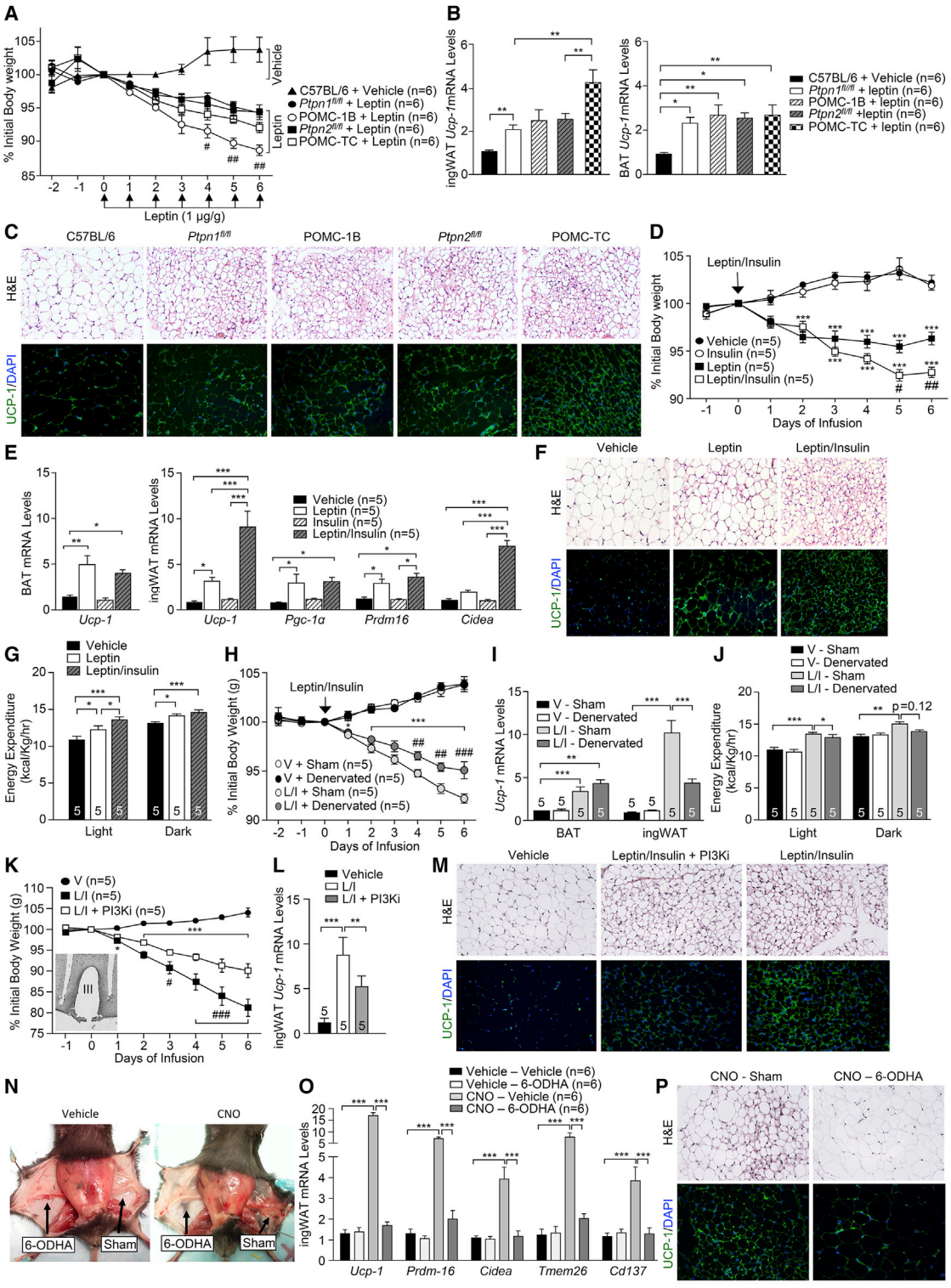

Figure 7. Leptin and Insulin Induce WAT Browning

(A–C) 8-week-old mice were administered leptin IP; (A) daily body weights were recorded; (B and C) ingWAT and BAT were extracted for (B) analysis of *Ucp-1* gene expression, (C) histology, and immunohistochemistry; C57BL/6 mice were administered vehicle as a control.

(D–G) 8-week-old C57BL/6 mice were ICV infused with vehicle, insulin (3 mU/day), leptin (4.8 μg/day), or insulin plus leptin, and (D) body weights monitored. (E and F) BAT and ingWAT were extracted for (E) gene expression analyses, (F) histology, and immunohistochemistry, and (G) energy expenditure was assessed.

(legend continued on next page)

from fat; SF04-027; Specialty Feeds) as indicated. Experiments were approved by the Monash University School of Biomedical Sciences Animal Ethics Committee.

Immunohistochemistry

Immunohistochemistry to monitor for p-STAT3 and p-AKT in hypothalamic neurons was performed as described previously (Loh et al., 2011), and staining for TCPTP, PTP1B, eGFP, and POMC was performed as described in the Extended Experimental Procedures. For inguinal WAT immunohistochemistry, tissue was formalin-fixed and processed for UCP-1, CD34, or TH immunoreactivity as described in the Extended Experimental Procedures.

Metabolic Measurements

Insulin and glucose tolerance tests, leptin sensitivity, blood glucose, and plasma insulin measurements were performed as described previously (Loh et al., 2009). Activity, food intake, and energy expenditure were assessed using a Comprehensive Lab Animal Monitoring System (Columbus Instruments), and body composition was assessed by DEXA (Lunar PIXImus2; GE Healthcare).

Real-Time PCR

RNA was extracted using TRIzol reagent (Sigma), reverse transcribed, and processed for quantitative (ΔΔCt) real-time PCR using either TaqMan Gene Expression Assays (Applied Biosystems) or SsoAdvanced Universal SYBR Green Supermix (BioRad) as described in the Extended Experimental Procedures.

BAT and Core Temperature Measurements

BAT and core temperatures and locomotor activity were measured as described previously (Enriori et al., 2011). E-Mitters (Mini Mitter Company) were implanted beneath the BAT pad between the scapulae or into the peritoneal cavity.

Sympathetic Denervation

Mice received 20 microinjections of vehicle or 6-hydroxydopamine [6-OHDA (Sigma); 1 μl per injection, 9 mg/ml in 0.15 M NaCl containing 1% (w/v) ascorbic acid] as described previously (Chao et al., 2011) throughout the right or both inguinal fat pads.

Intracerebroventricular and Intra-ARC Infusions

For intracerebroventricular infusions, 8-week-old C57BL/6 mice were implanted with a sterile osmotic pump connector cannula (Alzet Brain Infusion Kit 3, DURECT Corp) as described in the Extended Experimental Procedures. For intra-ARC infusions, mice were implanted with a bilateral cannula (Plastics One) 1.4 mm caudal of bregma, extending 5.7 mm below dura, connected to a minipump (Alzet model 1002, DURECT Corp) via PEG tubing and a Y connector. Mice received 6 day infusions of vehicle, leptin (4.8 μg/day, Peprotech), human insulin (3 mU/day, Sigma), or leptin plus insulin. Body weights and food intake were monitored, and tissues were extracted.

DREADD

10- to 12-week-old *Pomc*-Cre mice were sterotaxically injected with rAAV-hSyn-DIO-hM3D(Gq)-mCherry bilaterally into the ARC (coordinates, bregma: anterior-posterior, –1.40 mm; dorsal-ventral, –5.80 mm; lateral, +/–0.30 mm, 200 nl/side) as described previously (Krashes et al., 2011). Two weeks after rAAV delivery, mice were unilaterally denervated with 6-OHDA. One week postdenervation, mice received daily injections of vehicle or CNO (1.5 mg/kg, IP, Sigma) for 14 days. Body weights and food intake were recorded. Mice were anaesthetized, tissues were extracted, and mice were perfused with paraformaldehyde for immunohistochemical assessment.

Statistical Analysis

Unless otherwise indicated, statistical significance was determined by a two-tailed paired Student's t test. p values < 0.05 were considered significant; * or $^{\#}$ $p < 0.05$, ** or $^{\#\#}$ $p < 0.01$, and *** or $^{\#\#\#}$ $p < 0.001$.

SUPPLEMENTAL INFORMATION

Supplemental Information includes Extended Experimental Procedures and seven figures and can be found with this article online at http://dx.doi.org/10.1016/j.cell.2014.12.022.

ACKNOWLEDGMENTS

This work was supported by the NHMRC of Australia (to T.T., Z.B.A., and M.A.C.); the NIH to B.G.N. (R37-CA49152), Z.-Y.Z. (RO1-CA69202), K.K.B. (RO1-DK082417), and B.B.K. (RO1-DK98002); and funds from the Ontario Ministry of Health and Long Term Care and the Princess Margaret Cancer Foundation (B.G.N.).

Received: May 29, 2014
Revised: October 14, 2014
Accepted: December 10, 2014
Published: January 15, 2015

REFERENCES

Balthasar, N., Coppari, R., McMinn, J., Liu, S.M., Lee, C.E., Tang, V., Kenny, C.D., McGovern, R.A., Chua, S.C., Jr., Elmquist, J.K., and Lowell, B.B. (2004). Leptin receptor signaling in POMC neurons is required for normal body weight homeostasis. Neuron *42*, 983–991.

Banno, R., Zimmer, D., De Jonghe, B.C., Atienza, M., Rak, K., Yang, W., and Bence, K.K. (2010). PTP1B and SHP2 in POMC neurons reciprocally regulate energy balance in mice. J. Clin. Invest. *120*, 720–734.

Bartelt, A., Bruns, O.T., Reimer, R., Hohenberg, H., Ittrich, H., Peldschus, K., Kaul, M.G., Tromsdorf, U.I., Weller, H., Waurisch, C., et al. (2011). Brown adipose tissue activity controls triglyceride clearance. Nat. Med. *17*, 200–205.

Bence, K.K., Delibegovic, M., Xue, B., Gorgun, C.Z., Hotamisligil, G.S., Neel, B.G., and Kahn, B.B. (2006). Neuronal PTP1B regulates body weight, adiposity and leptin action. Nat. Med. *12*, 917–924.

Benoit, S.C., Air, E.L., Coolen, L.M., Strauss, R., Jackman, A., Clegg, D.J., Seeley, R.J., and Woods, S.C. (2002). The catabolic action of insulin in the brain is mediated by melanocortins. J. Neurosci. *22*, 9048–9052.

Berglund, E.D., Vianna, C.R., Donato, J., Jr., Kim, M.H., Chuang, J.C., Lee, C.E., Lauzon, D.A., Lin, P., Brule, L.J., Scott, M.M., et al. (2012). Direct leptin

(H–J) C57BL/6 mice were subjected to sham or ingWAT bilateral denervations (6-OHDA) and ICV infused with insulin + leptin. (H) Body weights, (I) BAT and ingWAT *Ucp-1* expression, and (J) energy expenditure were monitored.

(K–M) C57BL/6 mice were implanted with bilateral intra-ARC cannulas and infused with vehicle, insulin (3 mU/day) + leptin (4.8 μg/day), or insulin + leptin + PI3K inhibitor (PI3Ki; LY294002, 5 μg/day). (K) Daily body weights were recorded (insert: intra-ARC cannula placement) and ingWAT extracted for (L) analysis of *Ucp-1* gene expression, (M) histology, and UCP-1 immunohistochemistry.

(N–P) *Pomc*-Cre mice were bilaterally injected with rAAV-hSyn-DIO-hM3D(Gq)-mCherry into the ARC. Contralateral ingWAT depots were sham operated or denervated, and the mice were administered vehicle or CNO (1.5 mg/kg/day, IP) and ingWAT processed for (N) in situ morphology, (O) gene expression analysis, (P) histology, and immunohistochemistry.

Data are means ± SEM and are representative of three independent experiments; significance was determined using (A, D, H, and K) two-way ANOVA with repeated measures or (B, E, G, I, J, L, and O) one-way ANOVA. In (A), the pound (#) corresponds to $Ptpn1^{fl/fl}$ + Leptin versus POMC-1B + Leptin. In (D and H), the asterisk (*) corresponds to leptin(L) or L/insulin(I) versus vehicle (V), and the pound (#) L/I versus L or L/I + sham versus L/I + denervation. In (K), the asterisk (*) corresponds to L/I, or L/I + PI3Ki versus V, and the pound (#) L/I versus L/I + PI3Ki.

action on POMC neurons regulates glucose homeostasis and hepatic insulin sensitivity in mice. J. Clin. Invest. *122*, 1000–1009.

Boström, P., Wu, J., Jedrychowski, M.P., Korde, A., Ye, L., Lo, J.C., Rasbach, K.A., Boström, E.A., Choi, J.H., Long, J.Z., et al. (2012). A PGC1-α-dependent myokine that drives brown-fat-like development of white fat and thermogenesis. Nature *481*, 463–468.

Brüning, J.C., Gautam, D., Burks, D.J., Gillette, J., Schubert, M., Orban, P.C., Klein, R., Krone, W., Müller-Wieland, D., and Kahn, C.R. (2000). Role of brain insulin receptor in control of body weight and reproduction. Science *289*, 2122–2125.

Chao, P.T., Yang, L., Aja, S., Moran, T.H., and Bi, S. (2011). Knockdown of NPY expression in the dorsomedial hypothalamus promotes development of brown adipocytes and prevents diet-induced obesity. Cell Metab. *13*, 573–583.

Chiappini, F., Catalano, K.J., Lee, J., Peroni, O.D., Lynch, J., Dhaneshwar, A.S., Wellenstein, K., Sontheimer, A., Neel, B.G., and Kahn, B.B. (2014). Ventromedial hypothalamus-specific Ptpn1 deletion exacerbates diet-induced obesity in female mice. J. Clin. Invest. *124*, 3781–3792.

Cohen, P., Levy, J.D., Zhang, Y., Frontini, A., Kolodin, D.P., Svensson, K.J., Lo, J.C., Zeng, X., Ye, L., Khandekar, M.J., et al. (2014). Ablation of PRDM16 and beige adipose causes metabolic dysfunction and a subcutaneous to visceral fat switch. Cell *156*, 304–316.

Coll, A.P., Farooqi, I.S., Challis, B.G., Yeo, G.S., and O'Rahilly, S. (2004). Proopiomelanocortin and energy balance: insights from human and murine genetics. J. Clin. Endocrinol. Metab. *89*, 2557–2562.

Commins, S.P., Watson, P.M., Levin, N., Beiler, R.J., and Gettys, T.W. (2000). Central leptin regulates the UCP1 and ob genes in brown and white adipose tissue via different beta-adrenoceptor subtypes. J. Biol. Chem. *275*, 33059–33067.

Cowley, M.A., Smart, J.L., Rubinstein, M., Cerdán, M.G., Diano, S., Horvath, T.L., Cone, R.D., and Low, M.J. (2001). Leptin activates anorexigenic POMC neurons through a neural network in the arcuate nucleus. Nature *411*, 480–484.

Cypess, A.M., Lehman, S., Williams, G., Tal, I., Rodman, D., Goldfine, A.B., Kuo, F.C., Palmer, E.L., Tseng, Y.H., Doria, A., et al. (2009). Identification and importance of brown adipose tissue in adult humans. N. Engl. J. Med. *360*, 1509–1517.

Elias, C.F., Aschkenasi, C., Lee, C., Kelly, J., Ahima, R.S., Bjorbaek, C., Flier, J.S., Saper, C.B., and Elmquist, J.K. (1999). Leptin differentially regulates NPY and POMC neurons projecting to the lateral hypothalamic area. Neuron *23*, 775–786.

Enriori, P.J., Sinnayah, P., Simonds, S.E., Garcia Rudaz, C., and Cowley, M.A. (2011). Leptin action in the dorsomedial hypothalamus increases sympathetic tone to brown adipose tissue in spite of systemic leptin resistance. J. Neurosci. *31*, 12189–12197.

Hill, J.W., Williams, K.W., Ye, C., Luo, J., Balthasar, N., Coppari, R., Cowley, M.A., Cantley, L.C., Lowell, B.B., and Elmquist, J.K. (2008). Acute effects of leptin require PI3K signaling in hypothalamic proopiomelanocortin neurons in mice. J. Clin. Invest. *118*, 1796–1805.

Hill, J.W., Elias, C.F., Fukuda, M., Williams, K.W., Berglund, E.D., Holland, W.L., Cho, Y.R., Chuang, J.C., Xu, Y., Choi, M., et al. (2010). Direct insulin and leptin action on pro-opiomelanocortin neurons is required for normal glucose homeostasis and fertility. Cell Metab. *11*, 286–297.

Koch, L., Wunderlich, F.T., Seibler, J., Könner, A.C., Hampel, B., Irlenbusch, S., Brabant, G., Kahn, C.R., Schwenk, F., and Brüning, J.C. (2008). Central insulin action regulates peripheral glucose and fat metabolism in mice. J. Clin. Invest. *118*, 2132–2147.

Könner, A.C., Janoschek, R., Plum, L., Jordan, S.D., Rother, E., Ma, X., Xu, C., Enriori, P., Hampel, B., Barsh, G.S., et al. (2007). Insulin action in AgRP-expressing neurons is required for suppression of hepatic glucose production. Cell Metab. *5*, 438–449.

Krashes, M.J., Koda, S., Ye, C., Rogan, S.C., Adams, A.C., Cusher, D.S., Maratos-Flier, E., Roth, B.L., and Lowell, B.B. (2011). Rapid, reversible activation of AgRP neurons drives feeding behavior in mice. J. Clin. Invest. *121*, 1424–1428.

Lee, P., Linderman, J.D., Smith, S., Brychta, R.J., Wang, J., Idelson, C., Perron, R.M., Werner, C.D., Phan, G.Q., Kammula, U.S., et al. (2014). Irisin and FGF21 are cold-induced endocrine activators of brown fat function in humans. Cell Metab. *19*, 302–309.

Lidell, M.E., Betz, M.J., Dahlqvist Leinhard, O., Heglind, M., Elander, L., Slawik, M., Mussack, T., Nilsson, D., Romu, T., Nuutila, P., et al. (2013). Evidence for two types of brown adipose tissue in humans. Nat. Med. *19*, 631–634.

Loh, K., Deng, H., Fukushima, A., Cai, X., Boivin, B., Galic, S., Bruce, C., Shields, B.J., Skiba, B., Ooms, L.M., et al. (2009). Reactive oxygen species enhance insulin sensitivity. Cell Metab. *10*, 260–272.

Loh, K., Fukushima, A., Zhang, X., Galic, S., Briggs, D., Enriori, P.J., Simonds, S., Wiede, F., Reichenbach, A., Hauser, C., et al. (2011). Elevated hypothalamic TCPTP in obesity contributes to cellular leptin resistance. Cell Metab. *14*, 684–699.

Marino, J.S., Xu, Y., and Hill, J.W. (2011). Central insulin and leptin-mediated autonomic control of glucose homeostasis. Trends Endocrinol. Metab. *22*, 275–285.

Mori, H., Hanada, R., Hanada, T., Aki, D., Mashima, R., Nishinakamura, H., Torisu, T., Chien, K.R., Yasukawa, H., and Yoshimura, A. (2004). Socs3 deficiency in the brain elevates leptin sensitivity and confers resistance to diet-induced obesity. Nat. Med. *10*, 739–743.

Morrison, S.F., Madden, C.J., and Tupone, D. (2014). Central neural regulation of brown adipose tissue thermogenesis and energy expenditure. Cell Metab. *19*, 741–756.

Myers, M.G., Cowley, M.A., and Münzberg, H. (2008). Mechanisms of leptin action and leptin resistance. Annu. Rev. Physiol. *70*, 537–556.

Ouellet, V., Routhier-Labadie, A., Bellemare, W., Lakhal-Chaieb, L., Turcotte, E., Carpentier, A.C., and Richard, D. (2011). Outdoor temperature, age, sex, body mass index, and diabetic status determine the prevalence, mass, and glucose-uptake activity of 18F-FDG-detected BAT in humans. J. Clin. Endocrinol. Metab. *96*, 192–199.

Plum, L., Belgardt, B.F., and Brüning, J.C. (2006). Central insulin action in energy and glucose homeostasis. J. Clin. Invest. *116*, 1761–1766.

Plum, L., Rother, E., Münzberg, H., Wunderlich, F.T., Morgan, D.A., Hampel, B., Shanabrough, M., Janoschek, R., Könner, A.C., Alber, J., et al. (2007). Enhanced leptin-stimulated Pi3k activation in the CNS promotes white adipose tissue transdifferentiation. Cell Metab. *6*, 431–445.

Qiu, J., Fang, Y., Rønnekleiv, O.K., and Kelly, M.J. (2010). Leptin excites proopiomelanocortin neurons via activation of TRPC channels. J. Neurosci. *30*, 1560–1565.

Qiu, J., Zhang, C., Borgquist, A., Nestor, C.C., Smith, A.W., Bosch, M.A., Ku, S., Wagner, E.J., Rønnekleiv, O.K., and Kelly, M.J. (2014). Insulin excites anorexigenic proopiomelanocortin neurons via activation of canonical transient receptor potential channels. Cell Metab. *19*, 682–693.

Rahmouni, K., Morgan, D.A., Morgan, G.M., Liu, X., Sigmund, C.D., Mark, A.L., and Haynes, W.G. (2004). Hypothalamic PI3K and MAPK differentially mediate regional sympathetic activation to insulin. J. Clin. Invest. *114*, 652–658.

Rosen, E.D., and Spiegelman, B.M. (2014). What we talk about when we talk about fat. Cell *156*, 20–44.

Rothwell, N.J., and Stock, M.J. (1979). A role for brown adipose tissue in diet-induced thermogenesis. Nature *281*, 31–35.

Ruan, H.B., Dietrich, M.O., Liu, Z.W., Zimmer, M.R., Li, M.D., Singh, J.P., Zhang, K., Yin, R., Wu, J., Horvath, T.L., and Yang, X. (2014). O-GlcNAc transferase enables AgRP neurons to suppress browning of white fat. Cell *159*, 306–317.

Saltiel, A.R., and Kahn, C.R. (2001). Insulin signalling and the regulation of glucose and lipid metabolism. Nature *414*, 799–806.

Seale, P., Conroe, H.M., Estall, J., Kajimura, S., Frontini, A., Ishibashi, J., Cohen, P., Cinti, S., and Spiegelman, B.M. (2011). Prdm16 determines the thermogenic program of subcutaneous white adipose tissue in mice. J. Clin. Invest. *121*, 96–105.

Shabalina, I.G., Petrovic, N., de Jong, J.M., Kalinovich, A.V., Cannon, B., and Nedergaard, J. (2013). UCP1 in brite/beige adipose tissue mitochondria is functionally thermogenic. Cell Rep. *5*, 1196–1203.

Sohn, J.W., Xu, Y., Jones, J.E., Wickman, K., Williams, K.W., and Elmquist, J.K. (2011). Serotonin 2C receptor activates a distinct population of arcuate pro-opiomelanocortin neurons via TRPC channels. Neuron *71*, 488–497.

Tiganis, T. (2013). PTP1B and TCPTP—nonredundant phosphatases in insulin signaling and glucose homeostasis. FEBS J. *280*, 445–458.

van Marken Lichtenbelt, W.D., Vanhommerig, J.W., Smulders, N.M., Drossaerts, J.M., Kemerink, G.J., Bouvy, N.D., Schrauwen, P., and Teule, G.J. (2009). Cold-activated brown adipose tissue in healthy men. N. Engl. J. Med. *360*, 1500–1508.

Varela, L., and Horvath, T.L. (2012). Leptin and insulin pathways in POMC and AgRP neurons that modulate energy balance and glucose homeostasis. EMBO Rep. *13*, 1079–1086.

Virtanen, K.A., Lidell, M.E., Orava, J., Heglind, M., Westergren, R., Niemi, T., Taittonen, M., Laine, J., Savisto, N.J., Enerbäck, S., and Nuutila, P. (2009). Functional brown adipose tissue in healthy adults. N. Engl. J. Med. *360*, 1518–1525.

Williams, K.W., Margatho, L.O., Lee, C.E., Choi, M., Lee, S., Scott, M.M., Elias, C.F., and Elmquist, J.K. (2010). Segregation of acute leptin and insulin effects in distinct populations of arcuate proopiomelanocortin neurons. J. Neurosci. *30*, 2472–2479.

Williams, K.W., Liu, T., Kong, X., Fukuda, M., Deng, Y., Berglund, E.D., Deng, Z., Gao, Y., Liu, T., Sohn, J.W., et al. (2014). Xbp1s in Pomc neurons connects ER stress with energy balance and glucose homeostasis. Cell Metab. *20*, 471–482.

Wu, J., Boström, P., Sparks, L.M., Ye, L., Choi, J.H., Giang, A.H., Khandekar, M., Virtanen, K.A., Nuutila, P., Schaart, G., et al. (2012). Beige adipocytes are a distinct type of thermogenic fat cell in mouse and human. Cell *150*, 366–376.

Xue, Y., Petrovic, N., Cao, R., Larsson, O., Lim, S., Chen, S., Feldmann, H.M., Liang, Z., Zhu, Z., Nedergaard, J., et al. (2009). Hypoxia-independent angiogenesis in adipose tissues during cold acclimation. Cell Metab. *9*, 99–109.

Zhang, S., Chen, L., Luo, Y., Gunawan, A., Lawrence, D.S., and Zhang, Z.Y. (2009). Acquisition of a potent and selective TC-PTP inhibitor via a stepwise fluorophore-tagged combinatorial synthesis and screening strategy. J. Am. Chem. Soc. *131*, 13072–13079.